

# Balancing Passenger Transport and Power Distribution: A Distributed Dispatch Policy for Shared Autonomous Electric Vehicles

Jake Robbennolt, Meiyi Li, Javad Mohammadi, Stephen D. Boyles

**Abstract**—Shared autonomous electric vehicles can provide on-demand transportation for passengers while also interacting extensively with the electric distribution system. This interaction is especially beneficial after a disaster when the large battery capacity of the fleet can be used to restore critical electric loads. We develop a dispatch policy that balances the need to continue serving passengers (especially critical workers) and the ability to transfer energy across the network. The model predictive control policy tracks both passenger and energy flows and provides maximum passenger throughput if any policy can. The resulting mixed integer linear programming problem is difficult to solve for large-scale problems, so a distributed solution approach is developed to improve scalability, privacy, and resilience. We demonstrate that the proposed heuristic, based on the alternating direction method of multipliers, is effective in achieving near-optimal solutions quickly. The dispatch policy is examined in simulation to demonstrate the ability of vehicles to balance these competing objectives with benefits to both systems. Finally, we compare several dispatch behaviors, demonstrating the importance of including operational constraints and objectives from both the transportation and electric systems in the model.

**Index Terms**—Shared Autonomous Electric Vehicles, Grid Resilience, Service Restoration, Alternating Direction Method of Multipliers, Maximum Throughput Dispatch

## I. INTRODUCTION

Advancements in shared mobility-on-demand services, vehicle automation, and electrification are reshaping the transportation landscape, enabling shared autonomous electric vehicles (SAEVs) to facilitate dynamic interaction between transportation networks and the electric grid [1, 2]. Such vehicles have the potential to reduce electricity demand and voltage fluctuation and improve reliability and resilience in the electric grid if charging and discharging schemes are collaboratively optimized [3, 4, 5, 6, 7]. However, though many studies on vehicle routing have neglected the impact of electric vehicles (EVs) on the grid by assuming infinite power availability [8, 9], research has shown that incorrectly managed EV charging could lead to power quality problems [10]. Appropriate control can negate these concerns and lead to benefits such as peak shaving and voltage and frequency control, particularly when vehicle-to-grid charging technology is employed [11]. Furthermore, integrating EVs with renewable energy sources has shown particular promise in helping align electricity demand and supply curves, increasing economic benefits, and improving resilience [12, 13]. As the SAEV fleet size must be large

to serve peak hour demand, the incorporation of constraints related to the energy grid can enable additional uses for these vehicles when they are not needed for transportation.

Beyond day-to-day operations, there are additional resilience benefits when strains are put on the electric grid [14]. Natural disasters can endanger the distribution system, causing equipment failures, blackouts, and even larger scale propagation of failures throughout the network [15]. In the event of electric outages, the extra battery capacity of SAEVs can be leveraged to continue providing power to affected areas, particularly critical facilities such as hospitals and shelters [16, 17, 14]. While some research has examined modifying bus routes to support grid restoration while maintaining transit operations [18], most work has focused on transportable energy storage systems (TESSs), which requires grid operators or government agencies to own and operate a fleet of dedicated vehicles that do not need to transport passengers but can be costly [3]. When SAEVs are used, the benefits to electric consumers must be weighed against the continued needs of transportation passengers who may continue to be reliant on the SAEV fleet after the disaster.

This study introduces a dispatch policy that coordinates the SAEV system with the distribution network. In our framework, the grid operator manages power dispatch while the vehicle dispatcher optimizes vehicle logistics. Unlike previous research, we acknowledge that even during disruptions to the power grid, vehicles will continue to serve passengers. With this in mind, our proposed model ensures that the integrated efforts of the vehicle dispatcher and power grid operator achieve a balanced approach to maintaining essential transportation services, particularly for critical workers, and supporting end-user power needs during system disruptions [19, 20]. This novel cooperative approach allows for joint predictive control and modeling of vehicle and power flows, allowing vehicles to provide services to the electric grid while still maximizing passenger throughput [21, 5, 22, 23]. Furthermore, we advance our methodology by developing a distributed solution approach that enables local decision-making with minimal communication. This approach addresses scalability, stability, privacy, and resilience concerns more effectively. This heuristic, based on the alternating direction method of multipliers (ADMM) [24] achieves near-optimal, dynamic solutions quickly. Our findings from simulations on multiple networks illustrate the ability of the proposed dispatch policy to harmonize the competing demands of transportation and power grids, ultimately highlighting the critical need to inte-

grate operational constraints and objectives from both sectors into the planning model.

## II. DISPATCH POLICY

We first consider the power and vehicle dispatch problem as a joint centralized optimization where the vehicle dispatcher and electric grid operator want to maximize their combined profits (see Figure 1). We formulate the problem as a single mixed integer linear program using a model predictive control framework. Within this framework, we must track vehicle movements, passenger and energy flows, and vehicle state of charge over time. This section presents the centralized optimization problem by splitting the constraints into four sets: constraints on passenger queuing, vehicle charging, grid topology, and power flow, before presenting the combined objective.

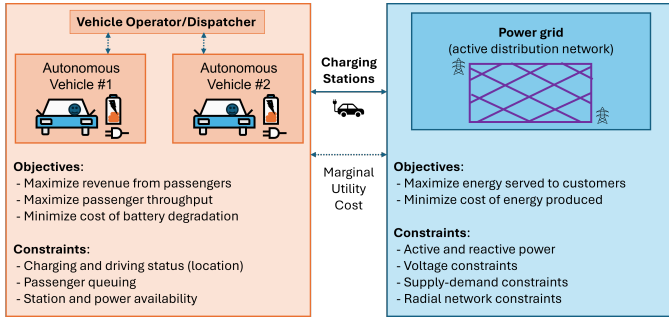


Fig. 1: Joint optimization between the fleet dispatcher and the electric grid operator.

Consider a roadway network  $\mathcal{G}_R = (\mathcal{N}_R, \mathcal{A}_R)$  and an electric network  $\mathcal{G}_E = (\mathcal{N}_E, \mathcal{A}_E)$  with nodes  $\mathcal{N}$  and links  $\mathcal{A}$ . We will use indices  $i$  and  $j$  to refer to nodes in the electric network and  $q, r$ , and  $s$  to refer to nodes in the transportation system. We also define a fleet of vehicles  $\mathcal{V}$ . We optimize vehicle dispatch through a model predictive control framework. At each timestep  $t$ , the optimization will run over the time horizon  $[t, t + \mathcal{T}]$  (we will use the notation  $t_\tau$  as a shorthand to refer to the time  $t + \tau$ ). Vehicles are controlled by the defined dispatch policy with decisions variables  $y_{qr}^v(t_\tau) \in \{0, 1\}$  (whether vehicle  $v$  will drive between nodes  $q$  and  $r$ ),  $Y_{qr}^v(t_\tau) \in \{0, 1\}$  (whether vehicle  $v$  pick up a passenger at  $q$  and take them to  $r$ ),  $\hat{\gamma}_{q,ch}^v(t_\tau) \in \{0, 1\}$ , and  $\hat{\gamma}_{q,dch}^v(t_\tau) \in \{0, 1\}$  (whether vehicle  $v$  will stay at node  $q$  to charge or discharge).

As vehicles can only be dispatched when they have completed a trip, these quantities are only defined when a vehicle is parked at node  $q$ . We define  $x_q^v(t_\tau) \in \{0, 1\}$  to denote whether a vehicle is parked at  $q$  at time  $(t_\tau)$ . Based on this setup, the vehicle conservation constraint for each vehicle  $v$  is:

$$\sum_{r \in \mathcal{N}_R} y_{qr}^v(t_\tau) + \hat{\gamma}_{q,ch}^v(t_\tau) + \hat{\gamma}_{q,dch}^v(t_\tau) \leq x_q^v(t_\tau), \quad \forall q \in \mathcal{N}_R, \forall v \in \mathcal{V}, \forall t_\tau \in \mathcal{T}. \quad (1)$$

Each vehicle can only choose a single action (drive, charge, or discharge) each time they are available for dispatch.

### A. Passenger Queuing Constraints

Passengers are tracked based on a queuing model, and vehicle and passenger movements are tracked across the time horizon.

We can constrain the dispatch of SAEVs traveling from  $q$  to  $r$  depending on whether vehicle  $v$  is actually parked at node  $q$ . To do this we define  $C_{qs}$  to be the travel time between nodes  $q$  and  $s$ . This travel time is assumed to be constant (not impacted by SAEV dispatch) but could include congestion. Then, vehicle state evolves as:

$$x_q^v(t_\tau + 1) = x_q^v(t_\tau) + \sum_{s \in \mathcal{N}_R} y_{sq}^v(t_\tau + 1 - C_{sq}) - \sum_{r \in \mathcal{N}_R} y_{qr}^v(t_\tau), \quad \forall q \in \mathcal{N}_R, \forall v \in \mathcal{V}, \forall t_\tau \in \mathcal{T}. \quad (2)$$

In general vehicles travel to the passenger pickup location and then take them to their destination, so the number of vehicles carrying passengers can be less than the total number of vehicles driving between nodes:

$$Y_{qr}^v(t_\tau) \leq y_{qr}^v(t_\tau), \quad \forall (q, r) \in \mathcal{N}_R^2, \forall v \in \mathcal{V}, \forall t_\tau \in \mathcal{T}. \quad (3)$$

We consider exogenous demand  $d_{qr}(t_\tau)$  to enter the network at node  $r$  with destination  $s$  at time  $(t_\tau)$ . These passengers form a separate queue  $w_{qr}(t_\tau)$  at each origin for each destination. Queues evolve within the model predictive control framework based on predicted future demand  $(\tilde{d}_{qr}(t_\tau))$ . Then,  $w_{qr}(t_\tau)$  evolves as follows:

$$w_{qr}(t + 1) = w_{qr}(t_\tau) + \tilde{d}_{qr}(t_\tau) - \sum_{v \in \mathcal{V}} Y_{qr}^v(t_\tau), \quad \forall (q, r) \in \mathcal{N}_R^2, \forall t_\tau \in \mathcal{T}. \quad (4)$$

Finally, the number of vehicles dispatched to serve passengers must be less than to total passenger demand:

$$\sum_{v \in \mathcal{V}} Y_{qr}^v(t_\tau) \leq w_{qr}(t_\tau), \quad \forall (q, r) \in \mathcal{N}_R^2, \forall t_\tau \in \mathcal{T}. \quad (5)$$

### B. Vehicle Charging Constraints

$\hat{\gamma}_{q,ch}^v(t_\tau) \in \{0, 1\}$  and  $\hat{\gamma}_{q,dch}^v(t_\tau) \in \{0, 1\}$  define whether vehicles are charging or discharging, but not how much power is being transferred. To track power flows, we define  $\gamma_{q,ch}^v(t_\tau) \in [0, 1]$  and  $\gamma_{q,dch}^v(t_\tau) \in [0, 1]$  and maximum charging and discharging rates  $\Gamma_{q,ch}^v$  and  $\Gamma_{q,dch}^v$ . We constrain power flows based on charging status and calculate the actual power taken from the grid based on the power flows:

$$\gamma_{q,ch}^v(t_\tau) \leq \hat{\gamma}_{q,ch}^v(t_\tau), \quad \forall q \in \mathcal{N}_R, \forall v \in \mathcal{V}, \forall t_\tau \in \mathcal{T}, \quad (6)$$

$$\gamma_{q,dch}^v(t_\tau) \leq \hat{\gamma}_{q,dch}^v(t_\tau), \quad \forall q \in \mathcal{N}_R, \forall v \in \mathcal{V}, \forall t_\tau \in \mathcal{T}, \quad (7)$$

$$ep_q^v(t_\tau) = \gamma_{q,ch}^v(t_\tau) \Gamma_{q,ch}^v - \gamma_{q,dch}^v(t_\tau) \Gamma_{q,dch}^v, \quad \forall q \in \mathcal{N}_R, \forall v \in \mathcal{V}, \forall t_\tau \in \mathcal{T}, \quad (8)$$

where  $ep_q^v(t_\tau)$  and  $eq_q^v(t_\tau)$  denote the active and reactive power that any individual vehicle parked at node  $q \in \mathcal{N}_R$  takes from or gives to the grid. As in Singh and Tiwari [25], we assume that EVs are equipped with bi-directional chargers that can inject/absorb reactive power without affecting the state of charge or battery life. Based on the active power taken from the grid, each vehicle is limited in the amount of reactive power that they can take [26, 27]. We can then constrain the reactive power flow based on a linear approximation of the real quadratic constraint (where  $\bar{e}s_q^v$  is the maximum allowed real power flow):

$$ep_q^v(t_\tau)^2 + eq_q^v(t_\tau)^2 \leq ([\hat{\gamma}_{q,ch}^v(t_\tau) + \hat{\gamma}_{q,dch}^v(t_\tau)] \bar{e}s_q^v)^2, \quad \forall q \in \mathcal{N}_R, \forall v \in \mathcal{V}, \forall t_\tau \in \mathcal{T}. \quad (9)$$

Recall that if  $[\hat{\gamma}_{q,ch}^v(t_\tau) + \hat{\gamma}_{q,dch}^v(t_\tau)] = 0$ , then no active or reactive power is allowed to be transferred through the charging station at  $q$ . The active power is already constrained by constraint (8), but this term constrains the reactive power as well. The linearization process is commonly used when constraining power flow through the distribution system [28, 29, 30, 3, 18].

Next, we need to ensure that any charging and discharging by vehicles at nodes in the roadway network is transferred to the electric grid. We define  $EP_i(t_\tau)$  and  $EQ_i(t_\tau)$  to be the amount of active and reactive power vehicles take (positive) or give (negative) to the grid at node  $i$ . The power distribution and transportation networks are connected by charging stations located at nodes, with connections denoted using the binary variable  $\delta_{qi} \in \{0, 1\}$  where  $i$  is in the electric grid and  $q$  is in the roadway network. Then, the values of power for individual vehicles need to be aggregated and converted to demands or supplies on the electric grid:

$$EP_i(t_\tau) = \sum_{q \in \mathcal{N}_R} \sum_{v \in \mathcal{V}} \delta_{qi} e p_q^v(t_\tau), \quad \forall i \in \mathcal{N}_E, \forall t_\tau \in \mathcal{T}, \quad (10)$$

$$EQ_i(t_\tau) = \sum_{q \in \mathcal{N}_R} \sum_{v \in \mathcal{V}} \delta_{qi} e q_q^v(t_\tau), \quad \forall i \in \mathcal{N}_E, \forall t_\tau \in \mathcal{T}. \quad (11)$$

We also need to ensure that vehicle are only allowed to charge and discharge if stations are available that their current node:

$$\sum_{v \in \mathcal{V}} [\hat{\gamma}_{q,ch}^v(t_\tau) + \hat{\gamma}_{q,dch}^v(t_\tau)] \leq N_q, \quad \forall q \in \mathcal{N}_R, \forall t_\tau \in \mathcal{T}, \quad (12)$$

where  $N_q$  is the number of charging stations at  $q$ .

For the vehicle energy tracking, we calculate the energy impacts of the dispatch decision as soon as vehicles are dispatched. Denote  $e^v(t_\tau)$  as the charge of vehicle  $v$  at time  $(t_\tau)$ , which can be updated as:

$$\begin{aligned} e^v(t_\tau + 1) &= e^v(t_\tau) - \sum_{(q,r) \in \mathcal{N}_R^2} y_{qr}^v(t_\tau) B_{qr} \\ &+ \sum_{q \in \mathcal{N}_R} \left[ \gamma_{q,ch}^v(t_\tau) \Gamma_{q,ch}^v - \frac{\gamma_{q,dch}^v(t_\tau) \Gamma_{q,dch}^v}{\eta_{q,dch}^v} \right], \end{aligned} \quad (13)$$

$\forall v \in \mathcal{V}, \forall t_\tau \in \mathcal{T},$

where  $B_{qs}$  is the energy requirements for traveling between  $q$  and  $s$ .

Once each vehicle's state of charge is known, it is straightforward to constrain it between some upper ( $\bar{e}^v$ ) and lower ( $\underline{e}^v$ ) bound:

$$\underline{e}^v \leq e^v(t_\tau) \leq \bar{e}^v, \quad \forall v \in \mathcal{V}, \forall t_\tau \in \mathcal{T}. \quad (14)$$

We assume  $\underline{e}^v$  is calculated based on the energy consumption needed to get to the nearest charging station.

### C. Grid Topology Constraints

The LinDistFlow power flow model described in Section II-D assumes a radial network, so the distribution system may need to be reconfigured [18, 31]. The variable  $u_{ij}(t_\tau) \in \{0, 1\}$  denotes the line state;  $u_{ij}(t_\tau) = 0$  if a line has failed. We also define  $s_{ij}(t_\tau) \in \{0, 1\}$  to indicate whether power flow should be allowed to flow.  $s_{ij}^d$  and  $s_{ji}^r$  are defined similarly for directed line flow between  $(i, j)$  and  $(j, i)$  respectively. Since power may only flow in one direction on each line, the topology is constrained by:

$$s_{ij}(t_\tau) \leq u_{ij}(t_\tau), \quad \forall (i, j) \in \mathcal{A}_E, \forall t_\tau \in \mathcal{T}, \quad (15)$$

$$s_{ij}(t_\tau) = s_{ij}^d(t_\tau) + s_{ji}^r(t_\tau), \quad \forall (i, j) \in \mathcal{A}_E, \forall t_\tau \in \mathcal{T}, \quad (16)$$

$$s_{j0}^r(t_\tau) = 0, \quad \forall j \in \mathcal{K}_G \cup \mathcal{K}_C, \forall t_\tau \in \mathcal{T}, \quad (17)$$

$$s_{0j}^d(t_\tau) = 1, \quad \forall j \in \mathcal{K}_G, \forall t_\tau \in \mathcal{T}, \quad (18)$$

$$s_{0j}^d(t_\tau) \leq 1, \quad \forall j \in \mathcal{K}_C, \forall t_\tau \in \mathcal{T}, \quad (19)$$

where the set  $\mathcal{K}_G$  is the set of source nodes connected to the grid.  $\mathcal{K}_C$  is the set of EV charging stations that can act as source nodes if disconnected from the grid but need not otherwise (the subset of  $\mathcal{N}_E$  that is attached to a charging station in  $\mathcal{N}_R$ ). Here, constraint (15) enforces the limitation

that power cannot flow on damaged lines. Constraint (16) ensures that power can only flow in one direction. Finally, constraints (17) and (18) require power flows from the virtual supersource while constraints (17) and (19) allow power flows from the virtual supersource.

We can also define the variable  $z_i(t_\tau) \in \{0, 1\}$  to represent the state of power supply of the distribution node. These variables, along with virtual demands  $f_i^L = 1$  for all nodes and virtual power flows  $f_{ij}$  allows us to construct the radial network:

$$\sum_{i \in \mathcal{N}_E: (i,k) \in \mathcal{A}_E} s_{ik}^d(t_\tau) + \sum_{j \in \mathcal{N}_E: (j,k) \in \mathcal{A}_E} s_{jk}^r(t_\tau) \leq 1, \quad (20)$$

$\forall k \in \mathcal{N}_E, \forall t_\tau \in \mathcal{T},$

$$\sum_{i \in \mathcal{N}_E: (i,k) \in \mathcal{A}_E} s_{ik}^d(t_\tau) + \sum_{j \in \mathcal{N}_E: (j,k) \in \mathcal{A}_E} s_{jk}^r(t_\tau) \geq z_k(t_\tau), \quad (21)$$

$\forall k \in \mathcal{N}_E, \forall t_\tau \in \mathcal{T},$

$$s_{ij}(t_\tau) - 1 \leq z_i(t_\tau) - z_j(t_\tau) \leq 1 - s_{ij}(t_\tau), \quad (22)$$

$\forall (i, j) \in \mathcal{N}_E^2, \forall t_\tau \in \mathcal{T},$

$$z_i(t_\tau) = \sum_{j \in \mathcal{N}_E} f_{ji}(t_\tau) - \sum_{j \in \mathcal{N}_E} f_{ij}(t_\tau), \quad (23)$$

$\forall i \in \mathcal{N}_E, \forall t_\tau \in \mathcal{T},$

$$-s_{ij}(t_\tau)N \leq f_{ij}(t_\tau) \leq s_{ij}(t_\tau)N, \quad (24)$$

$\forall (i, j) \in \mathcal{A}_E, \forall t_\tau \in \mathcal{T}.$

Constraint (20) requires the in-degree of each node to be less than or equal to 1 to ensure the network is radial. Constraint (21) ensures that each child node (powered) is assigned a single parent node. Constraint (22) enforces consistency between the state of each line and the state of the node on either side (if node  $i$  is powered by a source and  $j$  is not then the line between them cannot allow power to flow). Constraints (23) and (24) constitute flow conservation on the virtual network where  $N = |\mathcal{N}_E|$  is the number of distribution nodes.

### D. Power Flow Constraints

To model the power flow we use the LinDistFlow model [29, 30, 18] and assume that any fractional amount of load can be served. This is done using the variable  $l_i(t_\tau) \in [0, 1]$ . Based on network topology we can define:

$$l_i(t_\tau) \leq z_i(t_\tau), \quad \forall i \in \mathcal{N}_E, \forall t_\tau \in \mathcal{T}. \quad (25)$$

We can then define active and reactive power constraints to ensure we serve all demand ( $P_i^L(t_\tau)$  and  $Q_i^L(t_\tau)$  respectively) that has been chosen for pickup.

$$\sum_{j \in \mathcal{N}_E: (i,j) \in \mathcal{A}_E} P_{ij}(t_\tau) = P_i^G(t_\tau) - l_i(t_\tau)P_i^L(t_\tau) - EP_i(t_\tau), \quad (26)$$

$\forall i \in \mathcal{N}_E, \forall t_\tau \in \mathcal{T},$

$$\sum_{j \in \mathcal{N}_E: (i,j) \in \mathcal{A}_E} Q_{ij}(t_\tau) = Q_i^G(t_\tau) - l_i(t_\tau)Q_i^L(t_\tau) - EQ_i(t_\tau), \quad (27)$$

$\forall i \in \mathcal{N}_E, \forall t_\tau \in \mathcal{T}.$

The generated power  $P_i^G(t_\tau)$  and  $Q_i^G(t_\tau)$  is constrained within known limits:

$$\underline{P}_i^G \leq P_i^G(t_\tau) \leq \bar{P}_i^G, \quad \forall (i, j) \in \mathcal{A}_E, \forall t_\tau \in \mathcal{T}, \quad (28)$$

$$\underline{Q}_i^G \leq Q_i^G(t_\tau) \leq \bar{Q}_i^G, \quad \forall i \in \mathcal{N}_E, \forall t_\tau \in \mathcal{T}. \quad (29)$$

Next, the active and reactive power flows ( $P_{ij}(t_\tau)$  and  $Q_{ij}(t_\tau)$ ) must be bounded based on the real power constraint. This is done using the same linear approximation as above for

the constraint (where  $\bar{S}_{ij}$  is the maximum allowed real power):

$$P_{ij}(t_\tau)^2 + Q_{ij}(t_\tau)^2 \leq s_{ij}(t_\tau) \bar{S}_{ij}^2, \quad \forall (i, j) \in \mathcal{A}_E, \forall t_\tau \in \mathcal{T}. \quad (30)$$

Constraints (31) and (32) relate the voltage ( $V_i(t_\tau)$ ) to the power flows using the resistance  $R_{ij}$  and reactance  $X_{ij}$  of the lines. Then, constraints (33) and (34) set a constant voltage  $V_0$  for all nodes that supply power, and constrain the voltage between set bounds ( $\underline{V}_i$  and  $\bar{V}_i$ ) for all other nodes.

$$V_i(t_\tau) - V_j(t_\tau) \leq M(1 - s_{ij}(t_\tau)) + \frac{R_{ij}P_{ij}(t_\tau) + X_{ij}Q_{ij}(t_\tau)}{V_0}, \quad \forall (i, j) \in \mathcal{A}_E, \forall t_\tau \in \mathcal{T}, \quad (31)$$

$$V_i(t_\tau) - V_j(t_\tau) \geq M(s_{ij}(t_\tau) - 1) + \frac{R_{ij}P_{ij}(t_\tau) + X_{ij}Q_{ij}(t_\tau)}{V_0}, \quad \forall (i, j) \in \mathcal{A}_E, \forall t_\tau \in \mathcal{T}, \quad (32)$$

$$V_i(t_\tau) = V_0, \quad \forall i \in \mathcal{K}_G, \forall t_\tau \in \mathcal{T}, \quad (33)$$

$$z_i(t_\tau) \underline{V}_i \leq V_i(t_\tau) \leq z_i(t_\tau) \bar{V}_i, \quad \forall i \in \mathcal{N}_E \setminus \mathcal{K}_G, \forall t_\tau \in \mathcal{T}. \quad (34)$$

### E. Objective Function

In an ideal scenario, the dispatch policy ( $\pi^*$ ) would serve all passenger and electricity demand at every timestep. In this case, the goal should be to minimize either the total electricity consumption or the cost of electricity. However, this is unlikely to be the case in a disrupted network where vehicles may have competing demands from passengers and electric loads. In such a scenario, it makes more sense to *maximize* the profit or social welfare (which will also minimize electricity consumption/cost where possible). To do this we add up revenues from serving passengers and electric loads and subtract the cost of generating electricity and the cost of excessive charging and discharging of batteries. The objective function is as follows:

$$\begin{aligned} & \frac{1}{T} \sum_{\tau=1}^T \left[ \sum_{(r,s) \in \mathcal{N}_R^2} \mu_0(r, s, t) w_{rs}(t) \sum_{v \in \mathcal{V}} Y_{rs}^v(t_\tau) \right. \\ & + \sum_{(r,s) \in \mathcal{N}_R^2} \mu_1(r, s, t_\tau) \sum_{v \in \mathcal{V}} Y_{rs}^v(t_\tau) \\ & + \sum_{i \in \mathcal{N}_E} \mu_2(i, t_\tau) l_i(t_\tau) P_i^L(t_\tau) - \sum_{i \in \mathcal{N}_E} \mu_3(i, t_\tau) P_i^G(t_\tau) \\ & \left. - \sum_{v \in \mathcal{V}} \mu_4(v) \sum_{(q) \in \mathcal{N}_R} (\gamma_{q, ch}^v(t_\tau) \Gamma_{ch} + \gamma_{q, dch}^v(t_\tau) \Gamma_{dch}) \right]. \quad (35) \end{aligned}$$

In the objective (35), the  $\mu \geq 0$  functions are pricing functions set by the operator. Cost  $\mu_0$  is a demand responsive cost that should increase the payments by customers as demand in their queue increases. Cost  $\mu_1$  represents revenue from passengers once they are dropped at their destination based on distance or average travel times. Cost  $\mu_2$  represents revenue generated by payments for energy supplied to customers. Cost  $\mu_3$  is the price of generating energy. Finally, Cost  $\mu_4$  is the cost of battery degradation from charging and discharging. Since the initial queue lengths  $w_{rs}(t)$  are constant with respect to  $\pi^*$ , the final optimization problem is a mixed integer linear problem (assuming linear cost functions  $\mu$ ).

An important property of this objective function is that it ensures stability within the transportation network if it is possible (i.e. the expected number of waiting passengers remains bounded over time). The network is stable if there exists a  $\kappa < \infty$  such that

$$\lim_{T \rightarrow \infty} \frac{1}{T} \sum_{t=1}^T \sum_{(r,s) \in \mathcal{N}^2} \mathbb{E}[w_{rs}(t)] \leq \kappa.$$

The objective function proposed in Kang and Levin [21] for shared autonomous vehicle (SAV) dispatch is proven to stabilize demand if it is possible to do so. Note that within this electric vehicle framework the same is true. That proof relies on the first objective term (the demand responsive price) increasing to infinity if queues increase to infinity. This will eventually prioritize passenger service more than providing power to the electric grid and will ensure vehicles serve the longest queues first to maintain stability. For a more extensive discussion of this property and the impacts of electrification on stable dispatch, see Robbennolt [19].

### III. DISTRIBUTED DISPATCH

The model predictive control algorithm developed in the previous section is beneficial because it allows coordination between the power system and transportation system. Though this coordination is advantageous, it can make the problem substantially harder than solving each problem separately. In addition, though previous optimal dispatch strategies developed maximum throughput policies that did not need a time horizon and only tracked aggregate vehicle flows [5, 23], the need to track state of charge and provide real-time grid services means that individual vehicles must be tracked over a time horizon. Each of these complications increases the size of the problem, adding additional complexity.

In this section, we propose a distributed solution method which is scalable even for long time horizons and large fleet sizes and which also preserves privacy. In the decentralized algorithm, the vehicle dispatcher and power grid operator each solve their own problems, passing power flow estimates at charging stations and iterating until consensus (Figure 2). Section III-A will demonstrate that to solve the dispatch sub-problem, each vehicle will also solve its own lower-level optimization, passing passenger pickup and charging information to the vehicle dispatcher and iterating until convergence (Figure 3).

The distributed solution method proposed is based on ADMM, a well-established distributed optimization technique. Though ADMM cannot guarantee convergence of mixed-integer linear programs (MILPs), it is a useful heuristic since it allows the problem to be decomposed. At the upper level, while the integer variables defining dispatch remain fixed and the grid remains in a single radial configuration, the goal is to determine how much power SAEVs should take from the grid. This problem becomes a linear program (convex) when the integer routing and radial variables are fixed, so ADMM will converge exactly. While vehicles are switching routes, the discontinuities can cause issues with convergence. However, as the number of vehicles grows, these effects diminish, and the approximation improves. At the same time, as the problem grows (especially as the time horizon gets longer and the number of vehicles grows) the centralized problem becomes much more difficult to solve and the computational benefits of each vehicle optimizing its own route become more pronounced.

Many of the constraints in section II are separable by system (roadway or electric network). Constraints (10) and (11) aggregate the charge taken by vehicles from the grid, and

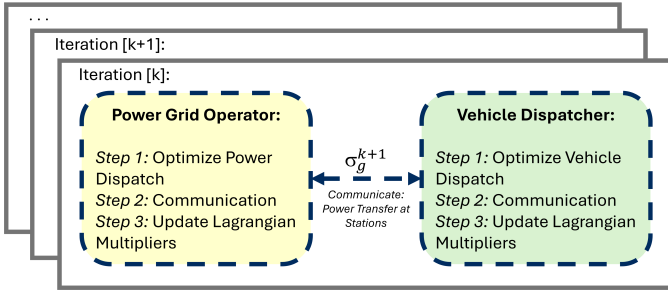


Fig. 2: Communications between power distribution system operator and SAEV dispatcher.

link the two problems. These constraints can be relaxed to form a separable problem. In order to create an algorithm to split the decisions of the vehicle dispatcher from the decisions of the power grid operator, each system can create a local copy of the variables  $EP_i(t_\tau)$  and  $EQ_i(t_\tau)$ . This will allow them to optimize their own system and choose the best values of these variables independently. Then, using *consensus* ADMM [24], a jointly optimal solution can be achieved. Rewrite the centralized problem as:

$$\min_{\sigma} \quad \text{Separable Objective: } f^R(\sigma) + f^E(\sigma), \quad (36a)$$

$$\text{s.t.} \quad \text{Separable Constraints R and E,} \quad (36b)$$

$$\sigma^R - \mu = 0, \quad \sigma^E - \mu = 0, \quad (36c)$$

where  $\sigma$  represents the estimate of the aggregate charge that vehicles take from the grid.  $\mu$  represents the consensus term that these estimates should converge to. The separable constraints are Equations (1) – (14) for the roadway network and Equations (15) – (34) for the power grid. This problem takes the form of a *consensus* ADMM problem with two agents (the power grid operator and the vehicle dispatcher) where  $EP_i(t_\tau)$  and  $EQ_i(t_\tau)$  have been replaced by their local copies  $EP_i^R(t_\tau)$  and  $EQ_i^R(t_\tau)$  in equations (10) and (11). In equations (26) and (27) they have been replaced by local copies  $EP_i^E(t_\tau)$  and  $EQ_i^E(t_\tau)$ .

We will define the index  $g$  to represent either the roadway  $R$  or electric networks  $E$  to simplify notation. Define  $\lambda_E^g$  as the Lagrangian multiplier associated with the consensus constraint and  $\rho_E$  as the ADMM penalty parameter. We refer to this penalty as  $\rho_E$  because it is associated with convergence of charging patterns based on fluctuations in the electric grid, though this parameter is used by the vehicle dispatcher as well to determine the relative benefit of providing power. The reason for this distinction will become clear in the next section. We also define the scaled dual variable  $u^g = \frac{\lambda^g}{\rho_E}$ , and the average of the two power flow estimates  $\bar{\sigma}$ . Then, this formulation simplifies to the iterative procedure of solving for  $\sigma^g$  and then updating the scaled dual variables (see Boyd et al. [24]):

$$\sigma_{k+1}^g = \underset{\sigma}{\operatorname{argmin}} \left[ f^g(\sigma^g) + \frac{\rho_E}{2} \|\sigma^g - \bar{\sigma}_k + u_k^g\|_2^2 \right], \quad (37)$$

$$\text{s.t.} \quad \text{Separable Constraints } g, \quad (37)$$

$$u_{k+1}^g = u_k^g + \sigma_{k+1}^g - \bar{\sigma}_{k+1}. \quad (38)$$

The optimization problem (37) can be solved separately by the vehicle dispatcher and power distribution system operator. Each system will determine optimal vehicle movements and power flows (respectively), and both systems will estimate the optimal power flow at charging stations. At each iteration  $k$ ,

only the information about predicted power flows at charging stations will be communicated, allowing each system to independently update their own Lagrangian multipliers and continue to the next iteration until convergence.

### A. Vehicle Dispatch Subproblem

The upper-level optimization results in two sub-problems, one for power flow optimizations and one for vehicle dispatch. We do not further simplify the power flow problem as it is generally easier to solve. However, the vehicle dispatch subproblem has many integer variables and remains difficult to solve quickly.

Based on the ADMM formulation in equation (37) and (38), we now formulate the vehicle dispatch subproblem (which must be solved at each iteration). The decision variables which relate vehicles to each other are the dispatch decisions to pick up passengers, as well as the decisions about the amount of power to take from the grid (referred to in aggregate as the vector  $z^v$  for each vehicle). Then, the lower-level vehicle dispatch problem can be written as:

$$\min_{z, \mu} \quad \sum_{v \in \mathcal{V}} f^v(z^v) + g \left( \sum_{v \in \mathcal{V}} z^v \right), \quad (39a)$$

$$\text{s.t.} \quad \text{Separable Constraints } v, \quad \forall v \in \mathcal{V}, \quad (39b)$$

$$h \left( \sum_{v \in \mathcal{V}} z^v \right) \leq \omega, \quad (39c)$$

where constraint (39b) includes all of the separable constraints that can be split between vehicles (equations (1), (6), (7), (2), (3), (8), (9), (13), and (14)). Constraint (39c) incorporates the non-separable constraints (4), (5), and (12). Constraints (10) and (11) can be dropped since we calculate the aggregate charge directly in the objective function. The first term in the objective is the separable constraints for the roadway network, each of which can also be separated for each vehicle. The second term is the function added by the upper-level ADMM, which requires consensus with the electric grid, so must account for the sum of all charging behaviors.

Note that this MILP includes a large number of integer variables, and the size of the problem still increases rapidly as the size of the roadway network increases. Further, this problem must be solved many times before the solution converges to the solution of problem (35), and the dispatch problem (35) must be solved at every timestep (every 15 seconds – 1 minute). This means the vehicle dispatch subproblem must be solved very quickly. To achieve a sufficiently fast solution we will again propose an ADMM approach, this time distributing subproblems to each vehicle while retaining a the vehicle dispatcher as a centralized coordinator (see figure 3). The inclusion of a term of the form  $\sum_{v \in \mathcal{V}} z_{qr}^v$  in the objective and constraints makes this problem a *sharing* problem which can be written in ADMM form by making a local copy of all shared variables [24]. To do this, replace  $z^v$  in optimization problem (39) with local copies  $\eta^v$  and then add the consensus constraint  $z^v - \eta^v = 0 \quad \forall v \in \mathcal{V}$ . Define  $\rho_R$  as the ADMM penalty parameter,  $\lambda^v$  as the Lagrange multipliers associated with ADMM constraint. As above,  $u^v$  is the scaled form of the Lagrangian multiplier  $\lambda^v$  ( $u^v = \frac{\lambda^v}{\rho_R}$ ). Also, based on the formulation by Boyd et al. [24], we replace  $\eta^v$  with  $\bar{\eta}$  for efficiency. Then, we can write the scaled form of ADMM as:

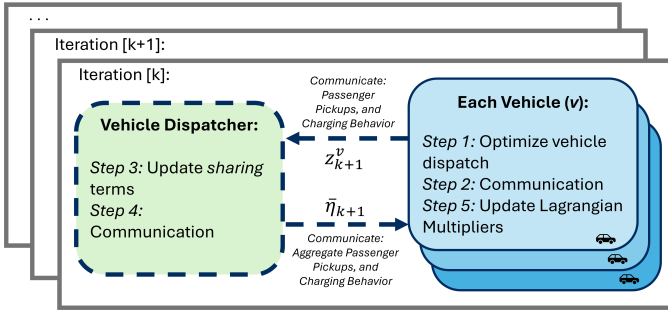


Fig. 3: Communications between vehicles and central controller.

$$z_{k+1}^v = \underset{z^v}{\operatorname{argmin}} \left[ f^v(z^v) + \frac{\rho_R}{2} \|z^v - z_k^v + \bar{z}_k - \bar{\eta}_k + u_k\|_2^2 \right], \quad (40a)$$

$$\text{s.t.} \quad \text{Separable Constraints } v, \quad \forall v \in \mathcal{V}, \quad (40b)$$

where  $z^v$  is updated independently and in parallel by each vehicle.

$$\bar{\eta}_{k+1} = \underset{\bar{\eta}}{\operatorname{argmin}} \left[ g(|\mathcal{V}|\bar{\eta}) + \frac{|\mathcal{V}|\rho_R}{2} \|\bar{\eta} - \bar{z}_{k+1} - u_k\|_2^2 \right], \quad (41a)$$

$$\text{s.t.} \quad h(|\mathcal{V}|\bar{\eta}) \leq \omega, \quad (41b)$$

where  $\bar{\eta}$  is the average of all local estimates  $\eta^v$  is update by the central controller.

$$u_{k+1} = u_k + \bar{z}_{k+1} - \bar{\eta}_{k+1}, \quad (42)$$

where  $u$  is updated by the central controller.

Finally, we clarify and further simplify the  $\bar{\eta}$  update. Recall that  $\eta^v$  is the local copy of the dispatch, so  $\bar{\eta}$  is the vectorization of all *shared* dispatch decisions ( $Y$ ,  $ep$ ,  $eq$ ,  $\hat{\gamma}_{ch}$ , and  $\hat{\gamma}_{dch}$ ). Since each of these appears independently in the constraints, the problem can be solved independently. As in the upper-level problem,  $\rho_R$  can be split by variable type. We define  $\rho_R^Y$ ,  $\rho_R^N$ ,  $\rho_R^p$ , and  $\rho_R^q$  as the penalty parameters associated with each decision variable type. Since vehicles share charging stations for both charging and discharging, both  $\hat{\gamma}_{ch}$  and  $\hat{\gamma}_{dch}$  must share  $\rho_R^N$ . Using this, we can split equation (41) into three parts.

First, constraint (24) states that the number of vehicles left to charge cannot exceed the number of charging stations. Then:

$$\bar{\eta}_{k+1}^{\hat{\gamma}_{ch}}, \bar{\eta}_{k+1}^{\hat{\gamma}_{dch}} = \underset{\bar{\eta}^{\hat{\gamma}_{ch}}, \bar{\eta}^{\hat{\gamma}_{dch}}}{\operatorname{argmin}} \left( \bar{\eta}^{\hat{\gamma}_{ch}} - \bar{z}_{k+1}^{\hat{\gamma}_{ch}} - u_k^{\hat{\gamma}_{ch}} \right)^2 + \left( \bar{\eta}^{\hat{\gamma}_{dch}} - \bar{z}_{k+1}^{\hat{\gamma}_{dch}} - u_k^{\hat{\gamma}_{dch}} \right)^2, \quad (43a)$$

$$\text{s.t.} \quad \bar{\eta}^{\hat{\gamma}_{ch}} + \bar{\eta}^{\hat{\gamma}_{dch}} \leq \frac{N}{|\mathcal{V}|}, \quad (43b)$$

where  $\bar{\eta}^{\hat{\gamma}_{ch}}$  and  $\bar{\eta}^{\hat{\gamma}_{dch}}$  must be updated jointly, but can be separated from the other variables and separated across each node  $q \in \mathcal{N}_R$  and each timestep  $\tau \in [0, \mathcal{T}]$ . Note that  $\rho_R^N$  must appear in equation (40) but can be dropped from (43).

Following similar logic, each  $\bar{\eta}^{ep}$  and  $\bar{\eta}^{eq}$  can be solved for independently for each node  $q \in \mathcal{N}_R$  and each timestep  $\tau \in [0, \mathcal{T}]$ :

$$\bar{\eta}_{k+1}^{ep} = \underset{\bar{\eta}^{ep}}{\operatorname{argmin}} \left[ g(|\mathcal{V}|\bar{\eta}^{ep}) + \frac{|\mathcal{V}|\rho_R^p}{2} (\bar{\eta}^{ep} - \bar{z}_{k+1}^{ep} - u_k^{ep})^2 \right], \quad (44a)$$

$$\bar{\eta}_{k+1}^{eq} = \underset{\bar{\eta}^{eq}}{\operatorname{argmin}} \left[ g(|\mathcal{V}|\bar{\eta}^{eq}) + \frac{|\mathcal{V}|\rho_R^q}{2} (\bar{\eta}^{eq} - \bar{z}_{k+1}^{eq} - u_k^{eq})^2 \right]. \quad (45a)$$

Finally, we consider the passenger service portion of the dispatch, estimated in aggregate by  $\bar{\eta}^{Y_{qr}}$ . This is constrained to be less than the queue of waiting passengers but is also used to create the queue length estimates at future timesteps. We rewrite constraints (4) and (5) in one equation as:

$$\sum_{v \in \mathcal{V}} \sum_{\tau=0}^{t'} Y_{qr}^v(t_\tau) \leq w_{qr}(t) + \sum_{\tau=0}^{t'} \tilde{d}_{qr}(t_\tau), \quad \forall (q, r) \in \mathcal{N}_R^2, \forall t' \in [0, \mathcal{T}], \quad (46)$$

where  $t'$  is an intermediate time between  $t$  and  $\mathcal{T}$ . The right-hand side of equation (46) is now a constant (since the initial queue length and exogenous demand estimates are known in advance). Then,  $\bar{\eta}^{Y_{qr}}$  can be updated as:

$$\bar{\eta}_{k+1}^{Y_{qr}} = \underset{\bar{\eta}^{Y_{qr}}}{\operatorname{argmin}} \left[ \|\bar{\eta}^{Y_{qr}} - \bar{z}_{k+1}^{Y_{qr}} - u_k^{Y_{qr}}\|_2^2 \right], \quad (47a)$$

$$\text{s.t.} \quad h(|\mathcal{V}|\bar{\eta}^{Y_{qr}}) \leq \omega_{qr}, \quad (47b)$$

where equation (47b) comes directly from (46). Note that this is a joint decision for all timesteps but can be separated for each node  $q \in \mathcal{N}_R$ . As in the  $\bar{\eta}^{\hat{\gamma}_{q,ch}}$  and  $\bar{\eta}^{\hat{\gamma}_{q,dch}}$  update,  $\rho_R^Y$  can be dropped from (47).

ADMM can then be performed by first running the optimization program (40) independently and in parallel for each vehicle. The vehicles must report their dispatch decisions ( $Y$ ,  $ep$ ,  $eq$ ,  $\hat{\gamma}_{ch}$ , and  $\hat{\gamma}_{dch}$ ). That is, the central controller must know which passengers are being picked up, when and where vehicles are parked to charge, and the amount of charge being taken or returned to the grid. Any other information such as routing, state of charge, passenger payments, etc. can be kept private. Next, the central controller updates all  $\bar{\eta}$  variables using equations (43), (44), (45), and (47). These can also be run in parallel, though they must be run by the central controller (not the individual vehicles). The results can be sent back to the vehicles for the Lagrangian multiplier update (42) and the next iteration can proceed until convergence.

## B. Convergence

To reiterate, the ADMM procedures developed in this section have no guarantees of convergence for the MILPs they are intended to solve. However, appropriate choices of the ADMM penalty terms as well as some other minor modifications to the problem allow the proposed algorithm to achieve high-quality solutions.

We have already discussed that each penalty term  $\rho$  can be separated based on variable type. This can be important when dealing with integer and continuous variables in the same problem. Since variables such as  $Y_{rs}^v(t)$  can be heavily impacted by small fluctuations in objective costs (both spatially and temporally) due to the nature of the vehicle's trajectory, large values of  $\rho_R^Y$  can cause very large changes in dispatch decisions across the entire fleet. On the other hand, given a stable dispatch solution, relatively values of  $\rho_E^p$  are needed to get vehicles to discharge back to the grid. These concerns are very important when using ADMM as a heuristic for the MILP,

so tuning is required to achieve fast and stable convergence to near-optimal solutions.

The relationship between variables in a Markovian structure (such as the queuing model used in vehicle dispatch) can make the convergence of the ADMM algorithm even harder. In general, for a single vehicle, an infeasibility at the end of the time horizon could require the entire route to be altered in the next iteration. However, the benefit of the model predictive control algorithm is that solutions at timesteps in the future are discarded. Thus, it is less important to achieve either optimality or feasibility at future times (particularly if future energy and passenger demands are not well known). For this reason, it is helpful to modify the penalty parameters  $\rho$  to be time-dependent. We define  $\rho(t) = \frac{\rho}{(\tau+1)^\alpha}$ , where  $\alpha$  is a small constant. This reduces the ADMM penalty over time, making large shifts to vehicle routing early in the time horizon less likely.

The other issue that arises when using this approach is that many vehicles may appear to be identical. Though this concern may be alleviated if vehicles are heterogeneous, it is possible that SAEVs in the future could become homogeneous (as they are in the case study below). In that case, vehicles starting from the same node with similar states of charge will always behave in exactly the same way. This can lead to cycling behavior of the algorithm as vehicles jump between two infeasible points repeatedly. This behavior has been documented in other problems such as the unit commitment problem [32]. Both cycling behavior and the issue of vehicle homogeneity can be solved by adding a proximal term  $\frac{\epsilon}{2}\|z^v - z_k^v\|_2^2$ . This is a special case of the term added by Zhang et al. [32]. However, instead of  $(z^v - z_k^v)^T P(z^v - z_k^v)$ , we use the  $L_2$  norm. We also define  $\epsilon$  as a vector, rather than a constant, where each element  $\epsilon^v$  is drawn from a random distribution  $U(0, \bar{\epsilon})$ . This serves to differentiate vehicles by their willingness to deviate from their current optimal solution. As the scaled dual variables change, the vehicle only switches routes when it is substantially more beneficial, and these decisions are made at different times based on the value of  $\epsilon^v$ . Generally, this should lead to more stable convergence, while still achieving similar solutions.

#### IV. NUMERICAL DEMONSTRATIONS

In this paper, we examine the properties of our dispatch strategy on a small but realistic network (5-node distribution system and 5-node transportation system with 10 SAEVs found in Robbennolt [19]). This allows for comparison between the centralized solution and the decentralized ADMM solution. To solve the centralized problems and the subproblems of the decentralized problem we use IBM ILOG CPLEX version 12.9. Additional tests are run on the larger Sioux Falls network (24 nodes) [33] using the IEEE-85 node network for the electric distribution system [34] with 150 SAEVs. A simulation model was created in Java to test to long term behavior of vehicles and collect queuing and energy service information. Simulations were run on a laptop computer with an Intel Core i7-1165 at 2.80 GHz and 16 GB of RAM.

Passengers are loaded based on a Poisson distribution and electric demands are perturbed around the mean using a

normal distribution (within 10%). We consider a contingency scenario in which approximately 35% (21% for the IEEE 85-node network) of the energy demand cannot be served from the grid and must be moved by vehicles. We consider vehicles acting as SAVs that do not discharge to the grid (but still must charge from the grid), TESSs that charge and discharge but do not serve passengers, and SAEVs dispatched using policy  $\pi^*$  (showcased in Figures 4 and 5). For the toy network, we also consider a scenario in which both types of vehicles are present, half SAVs and half TESSs. For this case study all of the pricing functions  $\mu$  are given a constant value except for  $\mu_1$  ( $\mu_0 = 1$  \$/pass,  $\mu_2 = 500$  \$/MWh,  $\mu_3 = 100$  \$/MWh, and  $\mu_4 = 50$  \$/MWh). We modify  $\mu_1$  to be discounted to encourage vehicles to be served more quickly:  $\mu_1 = 20 - \frac{0.1}{\tau+1}$  \$/hr.

The experiments on the toy network demonstrate that the combination of SAV services and grid restoration does not significantly reduce passenger service performance. Figure 4 shows that passenger queue lengths approximately double when vehicles also serve the grid. However, the service rate is less than the incoming demand rate (meaning in the long run all passengers will be served). In contrast, if only 5 vehicles serve passengers, the passenger queues will be unstable (eventually growing to infinity).

When comparing the cumulative unserved energy, the TESSs are able to serve almost all the energy demand. When only half the vehicles are available or when they are also being used for passenger service the performance is comparable. In these cases, there are some timesteps when all demand cannot be served (usually due to stochasticity and unexpected increases in the demand). In both cases if the vehicles focus on one system exclusively there are detriments to the other. SAVs serving passengers alone neglect 35% of the electric demand, and TESS serving passengers alone lead to unbounded passenger queues (and waiting times).

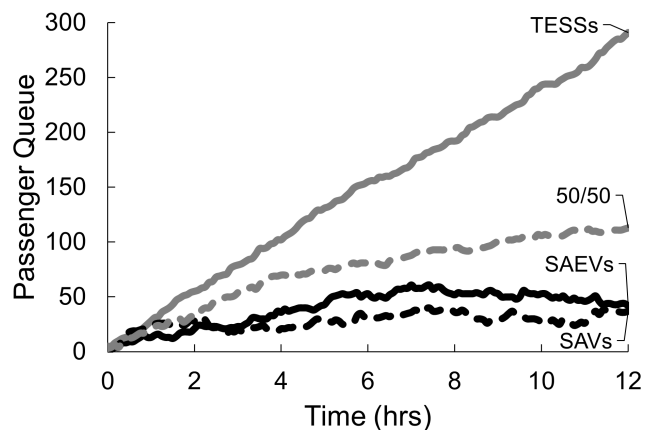


Fig. 4: Cumulative unserved passengers for different vehicle fleets. Queues are only stable for fleets of SAEVs and SAVs.

We next compare our decentralized ADMM algorithm with the centralized version using CPLEX. Examining the SAEV dispatch policy over the first three hours of operation in Figures 6 and 7, we can observe the process of queue formation and energy service. After three hours, both policies

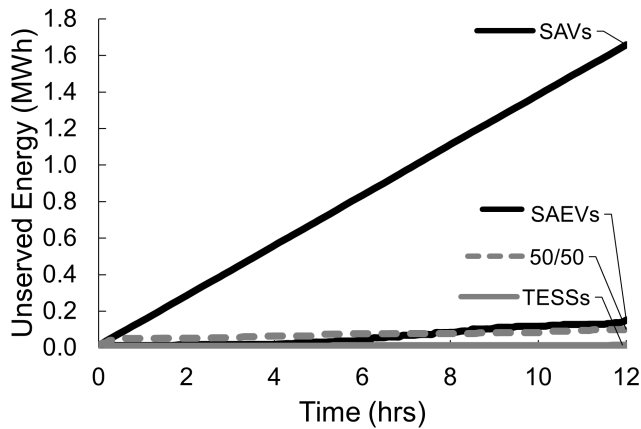


Fig. 5: Cumulative unserved energy (MWh) for different vehicle fleets. SAEVs and 50/50 fleets are able to serve almost all energy demand that cannot be served by the grid.

have stable passenger queues and serve approximately the same portion of the energy demand over time. These plots show that the decentralized policy is able to approximate the optimal solution, without high levels of communication. The passenger queues stabilize to similar queue lengths, and the energy service is only slightly lower. Additional heuristics built into the end of the process, ensuring vehicles are discharging at higher rates to serve all demand could be explored in the future to speed the convergence of the algorithm and reduce the difference between the two curves in Figure 7.

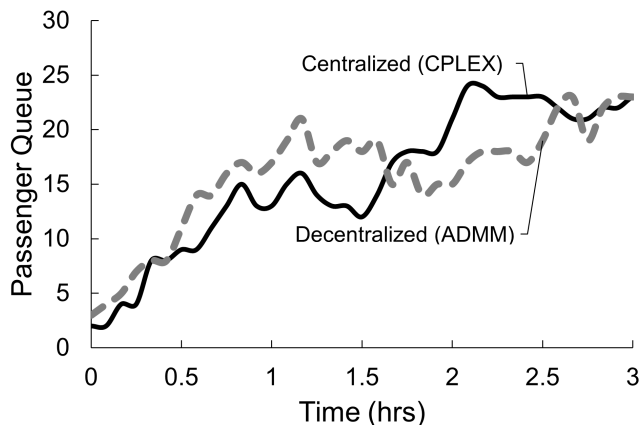


Fig. 6: Validation of ADMM algorithm based on cumulative unserved passengers. The decentralized method achieves queues that are comparable to the centralized approach.

We run similar tests on the larger Sioux Falls transportation network with the IEEE 85-node distribution network. These networks are shown in Figure 8 and are connected by four sets of charging stations. We test the operations of vehicles when used as SAV, TESSs, and SAEVs and there are two breaks in the electric grid between nodes 31–32 and nodes 34–44. Centralized solutions take hours (if they can be found at all) using the centralized problem in CPLEX, while good solutions can be found in 2–5 minutes using the decentralized ADMM approach (assuming vehicles can optimize their own routes in parallel). Additional speed gains can be found in the future by developing heuristics for the lower-level routing

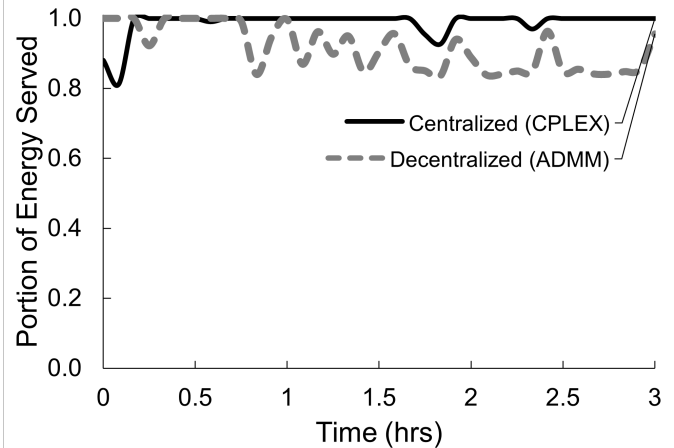


Fig. 7: Validation of ADMM algorithm based on cumulative unserved energy (MWh). The decentralized policy sometimes serves slightly less energy but is still able to serve almost all the demand.

problems.

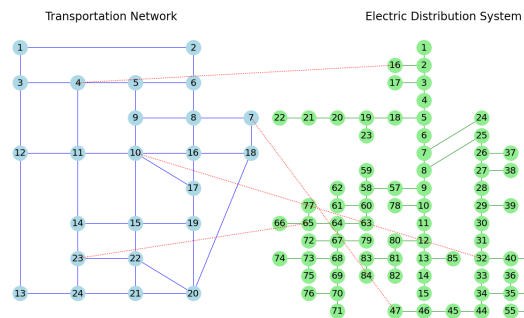


Fig. 8: Sioux Falls and IEEE 85-node networks connected by charging stations (red).

Figures 9 and 10 show a very similar pattern as for the smaller test network. The SAEVs are able to stabilize the demand with only slightly longer queues than if they were operated as SAVs, while also providing power to impacted areas. This is because vehicles already traveling between nodes carrying passengers can stop for a short time to discharge before carrying passengers the other direction and recharging. While neither fleet stabilizes passenger demands in the first 3 hours, the SAEV dispatch shows only slightly longer queues than that SAV fleet. These case studies suggest several implications for practical applications of SAEV routing methodologies and for future algorithmic improvements. This study suggests that ignoring interactions between SAEVs and the grid can be detrimental as charging and discharging behaviors add additional demands on the time of these vehicles. Ignoring such interactions could lead to underestimates of queue lengths as shown in Figures 4 and 9. On the other hand, ignoring the need to serve passengers (particularly during disaster scenarios) could lead to overestimates of the amount of power SAEVs can carry across outages (see figures 5 and 10). Though this paper focused on disaster scenarios, vehicles may also use vehicle to grid charging to reduce demand fluctuations, provide peak shaving, or many other grid services. However, demand fluctuations of energy and vehicles are linked, so this behavior needs to be better analyzed in a



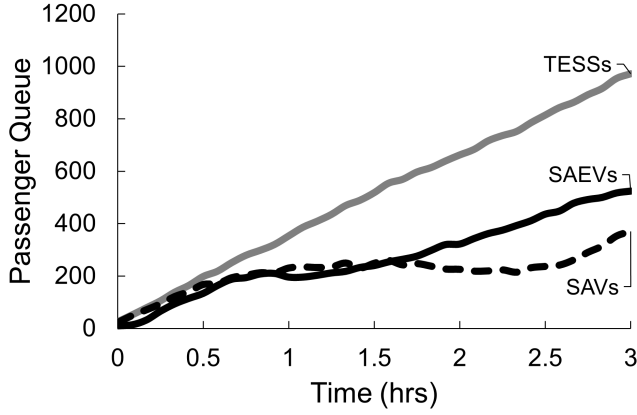


Fig. 9: Cumulative unserved passengers for different vehicle fleets. SAEVs have slightly longer queues than SAVs, though demand starts to stabilize after 3 hours for both fleets.

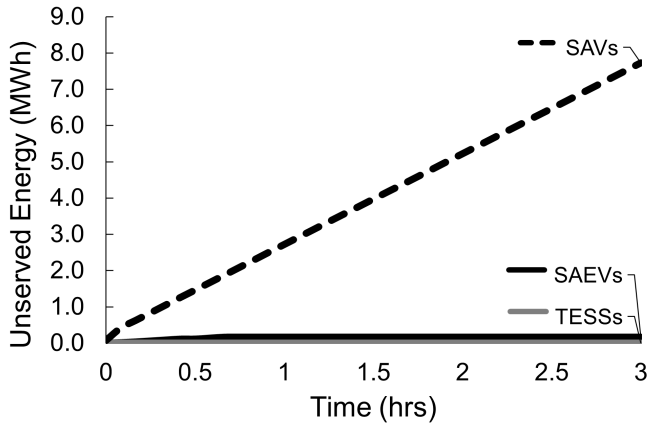


Fig. 10: Cumulative unserved energy (MWh) for different vehicle fleets. Both SAEVs and TESSs serve almost all of the energy demand.

comprehensive framework to understand these impacts.

When it comes to optimal dispatch, this work is built upon research into maximum throughput dispatch which ensures queues do not grow too large. The ADMM approach presented here actually presents some insight into this problem. When queues are very long, there are rarely conflicts when each vehicle takes its optimal path through the network (thus, computation times are relatively short). This aggregate behavior is exploited by previous approaches which do not need a time horizon and instead send vehicles to passengers with the longest head-of-line waiting time or with very short service times [5, 22, 23]. Though the SAEV dispatch proposed here relies on the time horizon, additional heuristics could be used to first route vehicles sequentially to achieve faster initial convergence to a feasible solution. When queues are shorter, there are more conflicts as many vehicles attempt to serve the same passengers (leading to much higher computation times). However, simple routing heuristics could be adopted in these cases since uncongested conditions are generally easier to solve with simple rules. Once the network becomes congested, the ADMM approach becomes increasingly easy to solve to near-optimal solutions as it also becomes increasingly valuable to find optimal routes.

## V. CONCLUSIONS

This paper examined the dispatch decision of SAEVs using the LinDistFlow model and a passenger queuing model. In the aftermath of a disaster these vehicles may be required to help serve critical electric loads while also providing mobility services for critical workers. While serving electric loads can improve resilience of the electric system, it can reduce the capacity of the vehicle fleet to serve passengers which could be detrimental for vulnerable populations. The model predictive control dispatch policy developed in this paper provides a framework for examining these competing objectives.

We also provide a heuristic based on ADMM which provides fast, near-optimal solutions to the problem. This approach becomes increasingly effective as the network becomes congested (an important benefit as this is the time when optimal dispatch is most important). Using this approach, we developed two case studies which demonstrate that ignoring potential demands on these vehicles could lead to an overestimation of the benefits to one system or the other. On the other hand, well optimized dispatch still leads to substantial benefits to both systems.

Future work should develop heuristics or use learning-based optimizers to solve the problem more quickly (for real-time implementation on realistic networks). The lower-level problems of the ADMM heuristic were solved with CPLEX, though many exhibit structures that could be exploited in additional exact or heuristic solution approaches. Additional research should also examine the sensitivity to the cost functions, fleet size, charging/discharging rate, length of the time horizon, and behavior under different loading scenarios (i.e. more realistic demand profiles). Similarly, additional objective functions should be tested for day-to-day operation that could minimize demand fluctuations, prioritize green energy sources, incorporate equity concerns, etc. In addition to better understanding the SAEV routing problem, we believe that our proposed ADMM heuristic could be applicable to other vehicle routing approaches. This subproblem was shown to be very effective when the network was congested, and variants could be applied to other large-scale dispatch and routing problems.

## REFERENCES

- [1] T. Unterluggauer, J. Rich, P. B. Andersen, and S. Hashemi, "Electric Vehicle Charging Infrastructure Planning for Integrated Transportation and Power Distribution Networks: A Review," *eTransportation*, vol. 12, p. 100163, May 2022.
- [2] D. J. Fagnant and K. Kockelman, "Preparing a Nation for Autonomous Vehicles: Opportunities, Barriers and Policy Recommendations," *Transportation Research Part A: Policy and Practice*, vol. 77, pp. 167–181, Jul. 2015.
- [3] S. Yao, P. Wang, and T. Zhao, "Transportable Energy Storage for More Resilient Distribution Systems With Multiple Microgrids," *IEEE Transactions on Smart Grid*, vol. 10, no. 3, pp. 3331–3341, May 2019.
- [4] S. Lei, J. Wang, C. Chen, and Y. Hou, "Mobile Emergency Generator Pre-Positioning and Real-Time Allocation for Resilient Response to Natural Disasters," *IEEE Transactions on Smart Grid*, vol. 9, no. 3, pp. 2030–2041, May 2018.
- [5] L. Li, T. Pantelidis, J. Y. J. Chow, and S. E. Jabari, "A Real-Time Dispatching Strategy for Shared Automated Electric Vehicles with Performance Guarantees," *Transportation Research Part*

- E: Logistics and Transportation Review*, vol. 152, p. 102392, Aug. 2021.
- [6] M. Mohammadi, J. Thornburg, and J. Mohammadi, "Towards an Energy Future with Ubiquitous Electric Vehicles: Barriers and Opportunities," *Energies*, vol. 16, no. 17, p. 6379, Jan. 2023.
  - [7] K. Nelson, J. Mohammadi, Y. Chen, E. Blasch, A. Aved, D. Ferris, E. A. Cruz, and P. Morrone, "Electric Vehicle Aggregation Review: Benefits and Vulnerabilities of Managing a Growing Fleet," in *2024 IEEE Texas Power and Energy Conference (TPEC)*, Feb. 2024, pp. 1–6.
  - [8] D. Goeke and M. Schneider, "Routing a Mixed Fleet of Electric and Conventional Vehicles," *European Journal of Operational Research*, vol. 245, no. 1, pp. 81–99, Aug. 2015.
  - [9] S. Pourazarm, C. G. Cassandras, and T. Wang, "Optimal Routing and Charging of Energy-Limited Vehicles in Traffic Networks," *International Journal of Robust and Nonlinear Control*, vol. 26, no. 6, pp. 1325–1350, 2016.
  - [10] G. A. Putrus, P. Suwanapongkarl, D. Johnston, E. C. Bentley, and M. Narayana, "Impact of Electric Vehicles on Power Distribution Networks," in *2009 IEEE Vehicle Power and Propulsion Conference*, Sep. 2009, pp. 827–831.
  - [11] J. Tomić and W. Kempton, "Using Fleets of Electric-Drive Vehicles for Grid Support," *Journal of Power Sources*, vol. 168, no. 2, pp. 459–468, Jun. 2007.
  - [12] H. Lund and W. Kempton, "Integration of Renewable Energy into the Transport and Electricity Sectors Through V2g," *Energy Policy*, vol. 36, no. 9, pp. 3578–3587, Sep. 2008.
  - [13] M. Moradijoo, M. Parsa Moghaddam, M. R. Haghifam, and E. Alishahi, "A Multi-Objective Optimization Problem for Allocating Parking Lots in a Distribution Network," *International Journal of Electrical Power & Energy Systems*, vol. 46, pp. 115–122, Mar. 2013.
  - [14] M. H. Amirioun, S. Jafarpour, A. Abdali, J. M. Guerrero, and B. Khan, "Resilience-Oriented Scheduling of Shared Autonomous Electric Vehicles: A Cooperation Framework for Electrical Distribution Networks and Transportation Sector," *Journal of Advanced Transportation*, vol. 2023, p. e7291712, Apr. 2023.
  - [15] S. Neumayer and E. Modiano, "Assessing the Effect of Geographically Correlated Failures on Interconnected Power-Communication Networks," in *2013 IEEE International Conference on Smart Grid Communications*, Oct. 2013, pp. 366–371.
  - [16] K. Rahimi and M. Davoudi, "Electric Vehicles for Improving Resilience of Distribution Systems," *Sustainable Cities and Society*, vol. 36, pp. 246–256, Jan. 2018.
  - [17] W. Sun, N. Kadel, I. Alvarez-Fernandez, R. R. Nejad, and A. Golshani, "Optimal Distribution System Restoration Using PHEVs," *IET Smart Grid*, vol. 2, no. 1, pp. 42–49, 2019.
  - [18] B. Li, Y. Chen, W. Wei, S. Huang, and S. Mei, "Resilient Restoration of Distribution Systems in Coordination With Electric Bus Scheduling," *IEEE Transactions on Smart Grid*, vol. 12, no. 4, pp. 3314–3325, Jul. 2021.
  - [19] J. Robbennolt, "Resilience and Operational Benefits of Electric Vehicle and Grid Integration," MSE, University of Texas at Austin, Austin, 2023.
  - [20] J. Robbennolt, J. Mohammadi, and S. D. Boyles, "Shared Autonomous Electric Vehicle Dispatch with Mobility and Distribution System Resilience Benefits," in *2024 IEEE Texas Power and Energy Conference (TPEC)*, Feb. 2024, pp. 1–6.
  - [21] D. Kang and M. W. Levin, "Maximum-Stability Dispatch Policy for Shared Autonomous Vehicles," *Transportation Research Part B: Methodological*, vol. 148, pp. 132–151, Jun. 2021.
  - [22] T. Xu, M. W. Levin, and M. Cieniawski, "A Zone-based Dynamic Queueing Model and Maximum-stability Dispatch Policy for Shared Autonomous Vehicles," in *2021 IEEE International Intelligent Transportation Systems Conference (ITSC)*, Sep. 2021, pp. 3827–3832.
  - [23] J. Robbennolt and M. W. Levin, "Maximum Throughput Dispatch for Shared Autonomous Vehicles Including Vehicle Rebalancing," *IEEE Transactions on Intelligent Transportation Systems*, pp. 1–15, 2023.
  - [24] S. Boyd, N. Parikh, E. Chu, B. Peleato, and J. Eckstein, "Distributed Optimization and Statistical Learning via the Alternating Direction Method of Multipliers," *Foundations and Trends® in Machine Learning*, vol. 3, no. 1, pp. 1–122, Jul. 2011.
  - [25] J. Singh and R. Tiwari, "Electric Vehicles Reactive Power Management and Reconfiguration of Distribution System to Minimise Losses," *IET Generation, Transmission & Distribution*, vol. 14, no. 25, pp. 6285–6293, 2020.
  - [26] M. C. Kisacikoglu, M. Kesler, and L. M. Tolbert, "Single-Phase On-Board Bidirectional PEV Charger for V2G Reactive Power Operation," *IEEE Transactions on Smart Grid*, vol. 6, no. 2, pp. 767–775, Mar. 2015.
  - [27] S. Pirouzi, J. Aghaei, M. A. Latify, G. R. Yousefi, and G. Mokryani, "A Robust Optimization Approach for Active and Reactive Power Management in Smart Distribution Networks Using Electric Vehicles," *IEEE Systems Journal*, vol. 12, no. 3, pp. 2699–2710, Sep. 2018.
  - [28] M. Baran and F. Wu, "Optimal Capacitor Placement on Radial Distribution Systems," *IEEE Transactions on Power Delivery*, vol. 4, no. 1, pp. 725–734, Jan. 1989.
  - [29] K. Turitsyn, P. Sulc, S. Backhaus, and M. Chertkov, "Distributed Control of Reactive Power Flow in a Radial Distribution Circuit with High Photovoltaic Penetration," in *IEEE PES General Meeting*, Jul. 2010, pp. 1–6.
  - [30] H.-G. Yeh, D. F. Gayme, and S. H. Low, "Adaptive VAR Control for Distribution Circuits With Photovoltaic Generators," *IEEE Transactions on Power Systems*, vol. 27, no. 3, pp. 1656–1663, Aug. 2012.
  - [31] N. Xin, L. Chen, L. Ma, and Y. Si, "A Rolling Horizon Optimization Framework for Resilient Restoration of Active Distribution Systems," *Energies*, vol. 15, no. 9, p. 3096, Jan. 2022.
  - [32] C. Zhang, L. Yang, and J. Jian, "Two-Stage Fully Distributed Approach for Unit Commitment with Consensus Admm," *Electric Power Systems Research*, vol. 181, p. 106180, Apr. 2020.
  - [33] T. N. for Research Core Team, "Transportation Networks for Research," Tech. Rep., accessed 2022-06-13. [Online]. Available: <https://github.com/bstabler/TransportationNetworks>
  - [34] O. D. Montoya, E. Rivas-Trujillo, and J. C. Hernández, "A Two-Stage Approach to Locate and Size PV Sources in Distribution Networks for Annual Grid Operative Costs Minimization," *Electronics*, vol. 11, no. 6, p. 961, Jan. 2022.